

Classification of strongly correlated f-electron systems

Frank Steglich, Christoph Geibel, Robert Modler, Michael Lang, Peter Hellmann, Philipp Gegenwart

Angaben zur Veröffentlichung / Publication details:

Steglich, Frank, Christoph Geibel, Robert Modler, Michael Lang, Peter Hellmann, and Philipp Gegenwart. 1995. "Classification of strongly correlated f-electron systems." *Journal of Low Temperature Physics* 99 (3-4): 267–81. <https://doi.org/10.1007/bf00752293>.

Nutzungsbedingungen / Terms of use:

licgercopyright

Dieses Dokument wird unter folgenden Bedingungen zur Verfügung gestellt: / This document is made available under these conditions:

Deutsches Urheberrecht

Weitere Informationen finden Sie unter: / For more information see:

<https://www.uni-augsburg.de/de/organisation/bibliothek/publizieren-zitieren-archivieren/publiz/>



Classification of Strongly Correlated f-Electron Systems

Frank Steglich, Christoph Geibel, Robert Modler, Michael Lang,
Peter Hellmann and Philipp Gegenwart

*Institut fuer Festkoerperphysik, Technische Hochschule Darmstadt, D-64289 Darmstadt,
Germany*

Ce-based heavy-fermion (HF) metals behave as Kondo-lattice systems and can be classified with the aid of a single coupling parameter, $|J|/W$, where $J < 0$ is the local exchange integral and W the conduction-band width. Depending on its actual composition, the exemplary material CeCu_2Si_2 chooses one out of two ground states: HF superconductivity and a new magnetic HF phase "A". In a narrow composition range, these two phases are nearly degenerate and expell each other upon varying either the temperature or the external magnetic field. The one-parameter-scaling approach appears inapplicable to the U-based HF metals. For the exemplary material UPd_2Al_3 , antiferromagnetic ordering between seemingly local 5f moments coexists, on a microscopic scale, with HF superconductivity. Whether this coexistence can be explained by assuming 5f states localized on a tetravalent U-ion with non-magnetic crystal-field ground state remains to be shown. We discuss arguments which invoke itinerant 5f states in the U-based HF metals to be distinguished from the localized 4f states in the Ce-based counterparts.

1. INTRODUCTION

Strongly correlated f-electron materials, i.e. periodic lattices of partially filled f shells in a metallic environment, can be classified with respect to two parameters characterizing the charge carriers: their concentration and the strength of their mutual interaction. Three different cases have been distinguished:¹ (i) Systems for which both of these quantities are relatively large (e.g., electron-doped cuprate superconductors^{2,3}), (ii) systems for which they both are relatively small (the so-called "low-carrier density lanthanide-based compounds"⁴) and (iii) "heavy-fermion" (HF) metals which exhibit a large concentration ($\sim 10^{22}\text{cm}^{-3}$) of only weakly correlated conduction electrons. In this paper we shall concentrate on these latter systems and discuss phenomenological similarities and differences between lanthanide- and actinide-based examples.

After briefly reviewing characteristic properties of HF metals in sect. 2, we shall address recent results on two exemplary systems which display very different

ground-state properties: CeCu_2Si_2 (sect. 3) and UPd_2Al_3 (sect. 4). These results are put into perspective in sect. 5.

2. SOME CHARACTERISTIC PROPERTIES OF 4f- AND 5f-ION-BASED HEAVY-FERMION METALS

HF metals can have different ground states which are commonly classified by adopting the magnetic limit of the periodic Anderson model, the so-called "Kondo lattice".⁵ In these materials, the formation of a local Kondo singlet (with binding energy $k_B T^* \sim \exp(W/J)$) competes with the formation of a cooperative magnetic state via the RKKY interaction (with binding energy $k_B T_{\text{RKKY}} \sim J^2/W$). Here, $J < 0$ is the local 4f/5f, conduction-electron exchange integral and W the width of the conduction band. For Ce systems, $|J|/W$ is raised upon volume compression.

At sufficiently small coupling parameter $|J|/W$, i.e. $T_{\text{RKKY}} > T^*$, local f-derived magnetic moments which can be substantially reduced by the Kondo effect form a cooperative magnetic state (hereafter termed local-moment magnetically ordered state, LMM). In most of these materials, a rather complex antiferromagnetic state is found.⁵ In general, substantially enhanced electronic specific heats γT , with $\gamma \sim 0.1 \text{ J/K}^2 \text{ mole}$, are detected below the Néel temperature T_N ; cf. the prototypical compounds CeAl_2 ⁶ and CeB_6 .⁷ In several of these compounds the electrical resistivity at $T < T_N$ contains an AT^2 contribution, where \sqrt{A} scales with the Sommerfeld coefficient γ according to the universal "Kadowaki-Wood plot".⁸ De-Haas-van-Alphen (dHvA) measurements typically reveal a low-temperature Fermi surface very similar to that of the corresponding La homologue.⁹⁻¹¹ Though apparently not reaching the large band masses as deduced from specific-heat experiments,¹¹ the cyclotron masses found in the dHvA experiments are markedly enhanced compared to those in the La homologues. All these observations indicate that the ordinary carriers of s, p or d symmetry are subject to an extraordinary mass renormalization by many-body effects operative in the low-T state of these magnetically ordered Kondo-lattice systems.

At sufficiently strong local exchange coupling, i.e. for $T^* > T_{\text{RKKY}}$, heavy Fermi liquids are observed at low temperatures, like in CeRu_2Si_2 ¹² and CeCu_6 .¹³ They are characterized by a large Sommerfeld coefficient of the electronic specific heat ($\gamma \sim 1 \text{ J/K}^2 \text{ mole}$), reflecting a gigantic quasiparticle mass $m^* (\simeq 100m_0 - 1000m_0; m_0 \text{ being the free-electron mass})$. Correspondingly huge Pauli spin susceptibilities are found, which contain additional information about the quasiparticle exchange interaction, accounted for by the Landau parameter $F_0^a: \chi \sim m^*/(1 + F_0^a)$. In spite of these enormous numbers their ratio, the Sommerfeld-Wilson ratio $R = (\chi/\mu_0\mu_{\text{eff}}^2)/(\gamma/(\pi^2 k_B^2)) = (1 + F_0^a)^{-1}$, is of order unity. A giant AT^2 term dominates the low-T electrical resistivity, and universal scaling $\sqrt{A} \sim \gamma$ is recovered again.⁸ dHvA experiments typically reveal a "large Fermi surface", i.e. a Fermi-surface volume exceeding that of the corresponding La homologue. In addition, recent studies on CeRu_2Si_2 ^{10,14} also revealed distinct anisotropies including light and heavy carrier masses ($4m_0 - 120m_0$). The latter have to be related to itinerant 4f electrons as predicted by "renormalized band-structure" calculations of the non-magnetic Kondo lattice.¹⁵ The transition from a "small" to a "large Fermi surface" is clearly evident when the dHvA results¹⁰ are compared for the two ho-

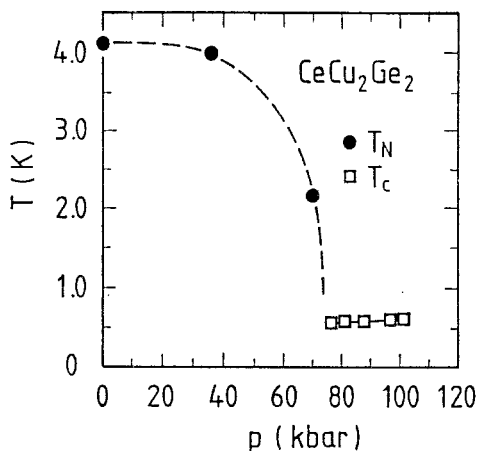


Fig. 1. Néel temperature and superconducting transition temperature of CeCu_2Ge_2 as a function of pressure (adapted from²⁰).

mologues CeRu_2Ge_2 , a ferromagnetic LMM compound with $T_{\text{RKKY}} \gg T^*$,¹⁶ and the heavy-Fermi-liquid system CeRu_2Si_2 exhibiting a considerably smaller unit-cell volume and $T^* > T_{\text{RKKY}}$: The electron-related Fermi surface of CeRu_2Ge_2 at low temperature is found to be smaller, its hole-related Fermi surface to be larger than that of CeRu_2Si_2 , and the difference between the two amounts to just one (4f) electron. This indicates that the 4f electron is localized in CeCu_2Ge_2 , but is itinerant in the Si homologue.

From the existence of a $T = 0$ K “Mott transition” between localized and itinerant f states, tantamount to a $T = 0$ K magnetic phase transition between a LMM phase and a heavy-Fermi-liquid phase with “large Fermi surface”, universal behavior of the latter has been deduced for $T < T_{\text{coh}} < T^*$.¹⁷ Here, T_{coh} marks the crossover between the coherent Fermi liquid at low and the paramagnetic regime of local f-derived moments at high temperature. Furtheron, it was recently demonstrated by dHvA experiments¹⁴ that, even at $T \ll T_{\text{coh}}$, the 4f electrons can be localized in CeRu_2Si_2 , namely by applying a sufficiently high magnetic field B: once B exceeds the “metamagnetic field” $B_m \simeq 8$ T, the “large Fermi surface” becomes replaced by the “small” one. The apparent break down of Fermi-liquid behavior associated with the abrupt change of the Fermi-surface volume at the critical coupling constant $(|J|/W)_c$ has recently been recognized as being one of the routes to “non-Fermi-liquid” phenomena.^{18,19}

The preceding survey suggests strongly that Ce-based HF metals can, in fact, be classified by a single coupling parameter, $|J|/W$. In particular, several Ce-based systems are known to show a magnetic instability at $T \simeq 0$ K. In fig. 1, Jaccard et al.’s²⁰ results on CeCu_2Ge_2 are displayed as an especially striking example. At ambient pressure, CeCu_2Ge_2 belongs to the class of LMM systems ($T^* \simeq T_{\text{RKKY}} \simeq$

7 K).²¹ If exerted to external pressure, p , the Néel temperature ($T_N = 4.1$ K at $p = 0$ kbar) starts to decrease, eventually vanishing for $p \gtrsim 70$ kbar. Note that this pressure is required to compress the unit-cell volume of CeCu_2Ge_2 to the $p = 0$ kbar volume of its Si homologue.¹⁹ Most interesting was the observation that in its non-magnetic high-pressure state, CeCu_2Ge_2 shows a superconducting transition at $T_c \simeq 0.64$ K,²⁰ strongly resembling the one in CeCu_2Si_2 at ambient pressure.²² A magnetic instability of the heavy-Fermi-liquid phase below $T = 1$ K was discovered in yet another member of the same family: Ni-rich $\text{Ce}(\text{Cu}_{1-x}\text{Ni}_x)_2\text{Ge}_2$.²¹ In sect. 3 we will address the B-T phase diagram of CeCu_2Si_2 in which different symmetry-broken HF states (i.e. a superconducting and a magnetic one) compete with and mutually expell each other.

CeCu_2Si_2 behaves completely differently from U-based HF metals which are usually showing coexistence between different symmetry-broken HF states. For example, for UPt_3 the superconducting regime at low temperature and low magnetic field is embedded in an antiferromagnetically ordered state with $T_N \simeq 6$ K $\simeq 10 T_c$. Both phenomena, which coexist below T_c ,²³ are of highly unusual type. HF superconductivity occurs in three different phases indicating an unconventional order parameter.²⁴ The saturated staggered antiferromagnetic moment is extremely small ($\sim 10^{-2} \mu_B$), while the ordering wave vector is large and commensurate.²³ A similar low-moment antiferromagnetic state ($T_N \simeq 17$ K) coexists with HF superconductivity in URu_2Si_2 below $T_c \simeq 1$ K.²⁵ For UNi_2Al_3 ($T_c = 1$ K, $T_N = 4.6$ K), too, such a scenario occurs,²⁶ however with a larger saturated moment, $\mu_0 \simeq 0.24 \mu_B$.²⁷

In sect. 4 we discuss the novel case of UPd_2Al_3 ,²⁸ for which HF superconductivity below $T_c = 2$ K coexists with antiferromagnetic ordering among $5f$ -derived moments as large as $\simeq 1 \mu_B$.²⁹ This antiferromagnetic phase appears phenomenologically closely related to the LMM phases found in Ce-based Kondo lattices. However, within the one-parameter-scaling scheme which appears applicable to the latter systems, coexistence on a microscopic scale between LMM and a heavy, f -derived Fermi-liquid phase (or one of its symmetry-broken states) is not possible, and an alternative scheme is required.

3. THE B-T PHASE DIAGRAM OF CeCu_2Si_2

The low-temperature ($T \leq 1$ K), magnetic field ($B \leq 16$ T) diagram of CeCu_2Si_2 contains several phases which do not seem to coexist with each other on a microscopic scale. Cu-NMR³⁰ as well as $B = 0$ T - μSR results³¹ indicate magnetic correlations to develop below $T \simeq 1.5$ K. These are precursive of a transition from the paramagnetic ("C") into a low-T magnetic phase ("A") which had already been observed several years ago in various techniques.³² Fig. 2 presents the B-T phase diagram as obtained by Bruls et al.³³ through measurements of the elastic constants, thermal expansion and magnetostriction. Both specific-heat^{34,35} and resistivity³⁶ experiments have been used to confirm this phase diagram, including the high-field phase "B". Bruls et al.'s motivation to perform their thorough study was the, at first glance, astonishing observation that the elastic constant (e.g. $c_{11}(B)$), when isothermally monitored as a function of decreasing B field, showed a positive jump at $B = B_c$, i.e. at the transition from phase A into the superconducting state. Since, according to Landau's theory, a negative discontinuity of the

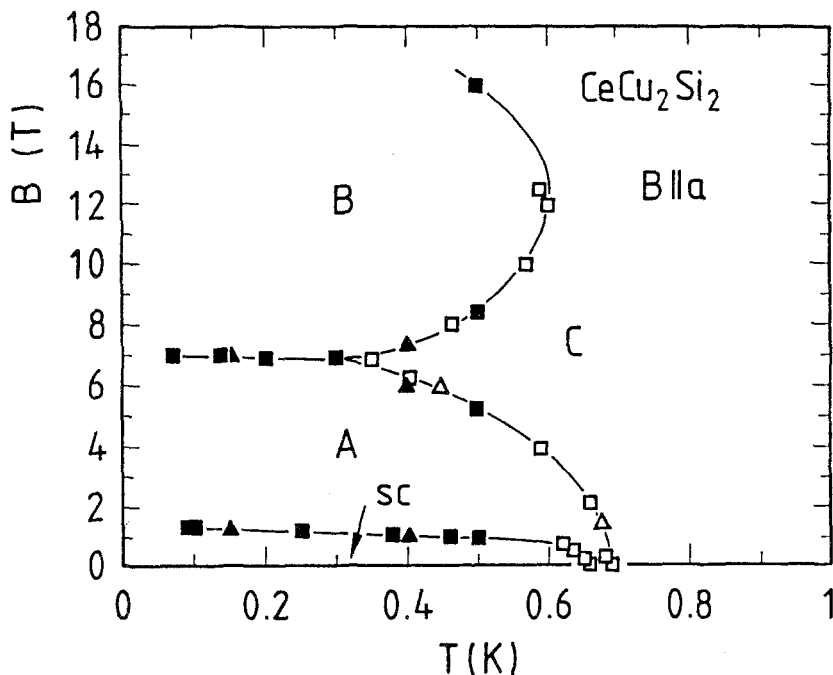


Fig. 2. B-T phase diagram of CeCu₂Si₂ single crystal (adapted from³³).

elastic constant is expected upon symmetry lowering, these authors concluded that the low-field transition manifests a replacement of phase A by superconductivity. This is directly observed via constant-field measurements in the temperature dependence of both the elastic constants,³³ and the thermal expansion, $\alpha(T)$ (fig. 3a): Upon cooling at zero field, the incipient C \rightarrow A transition is replaced by the A \rightarrow SC transition which occurs at $T_c \simeq 0.67$ K. Both the large positive jump anomaly and the T dependence of $\alpha(T)$ at lower temperature indicate that HF superconductivity develops in the bulk of this single crystal (cf. fig. 3b and the following discussion). In an overcritical B field of 1.5 T, superconductivity is suppressed and phase A fully recovered. The whole of the experimental observations have led to assume that superconductivity and phase A exist in disjunct parts of the B-T phase diagram.³³ Both states are nearly degenerate: previous studies revealed^{32,37} that a number of (unannealed) CeCu₂Si₂ single crystals did not show bulk superconductivity, but instead a bulk transition into phase A with an onset at $T_A \simeq 0.7$ K (and an additional low-T transition, probably of antiferromagnetic origin, fig. 3c). After annealing, however, in several of these crystals phase A was found absent at B fields below 5 T, while bulk superconductivity developed below $T_c(0) \simeq 0.63$ K and $B_{c2}(0) \gtrsim 2$ T, cf. fig. 3b. Note that this value of the upper critical field is substantially larger than for the crystal displayed in fig. 3a, which clearly demonstrates

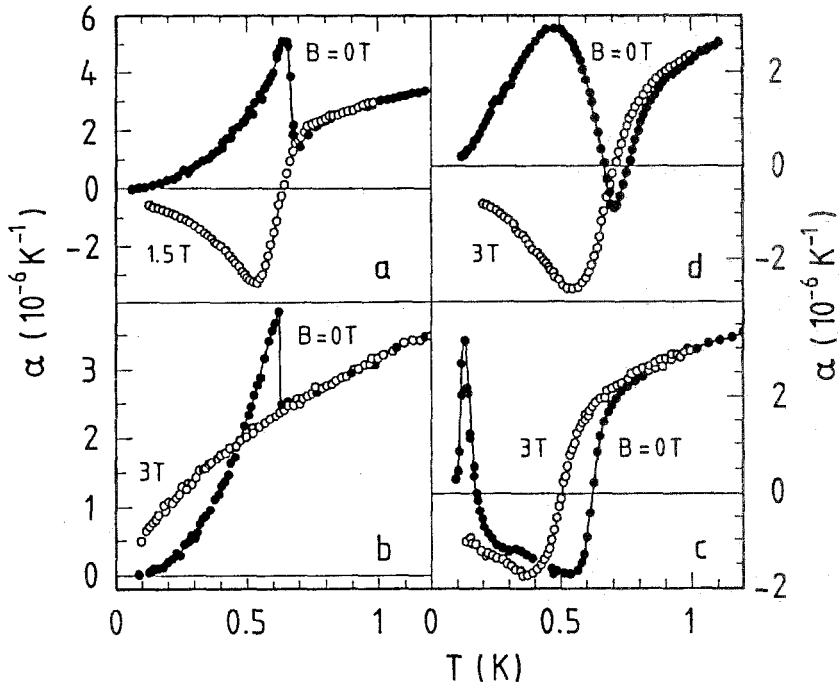


Fig. 3. Linear thermal-expansion coefficient as a function of temperature at both zero field and $B \gtrsim B_{c2}(0)$, with $B \parallel a$, for three CeCu_2Si_2 single crystals: a) same crystal as in fig. 2; b) superconducting crystal;³² c) non-bulk-superconducting crystal ("as grown").³² The low-T peak in the $B = 0$ T data in c) indicates an additional transition, probably of antiferromagnetic origin.³² In d) one third of the volume-thermal-expansion coefficient, $\alpha(T) = \frac{1}{3}\beta(T)$, at $B = 0$ T and 3 T is shown for a polycrystalline sample from the "border line" regime (see fig. 4).

a weakening of the thermodynamic stability of HF superconductivity in the vicinity of phase A.

In order to shed light onto this most extraordinary sample dependence of the ground-state properties in CeCu_2Si_2 , we have recently initiated an investigation of polycrystalline samples with composition in the vicinity of the "122" phase.³⁸ As a result of thermal-expansion and specific-heat measurements³⁸ as well as of simultaneous μSR investigations,³¹ we found Ce and/or Cu excess to stabilize superconductivity, in accord with previous reports,^{39,40} but Ce and/or Cu deficiency to stabilize the phase A, see fig. 4. Since one sample with a large volume content of phase A showed a particularly high density of microcracks, it was argued³¹ that this sample existed in a strain-released state. Therefore, phase A might be assumed to be as sensitive to internal strain as it is to external pressure.³² In the

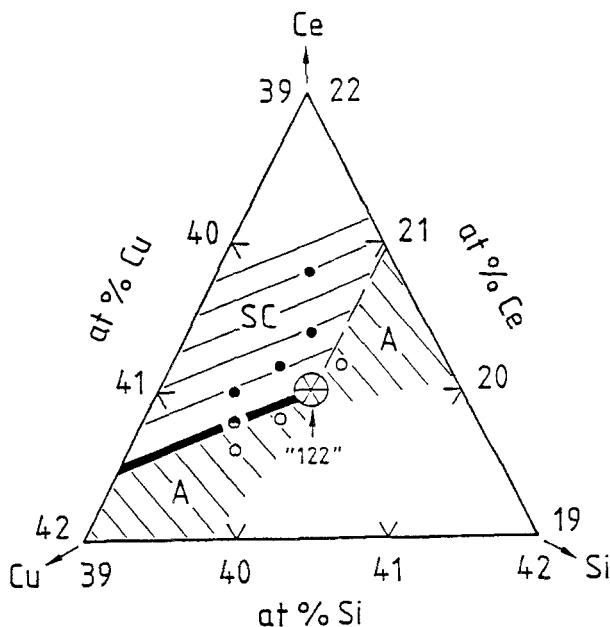


Fig. 4. Relation between composition and ground-state properties for $\text{Ce}_{1\pm x}\text{Cu}_{2\pm y}\text{Si}_2$ in the vicinity of the stoichiometric "122" composition. Stability ranges for superconductivity and phase A as well as "border-line" regime are indicated.⁵³

same type of reasoning, internal strain (caused by inhomogeneities in site occupation) may favor HF superconductivity to form in those parts of the sample in which phase A is suppressed. In fact, $B = 0 \text{ T} - \mu SR$ experiments on polycrystalline samples reveal the simultaneous occurrence, owing to unavoidable compositional fluctuations, of three "domains". These can be characterized (upon cooling) in the following manner: "domain 1" (paramagnetism \rightarrow superconductivity), "domain 2" (magnetic correlations \rightarrow phase A) and "domain 3" (magnetic correlations \rightarrow phase A \rightarrow superconductivity). The existence range of the latter domain appears to be rather narrow, i.e. to be confined to the border line between the superconducting and phase-A regimes in fig. 4. In fig. 3d, the thermal-expansion data are shown for a polycrystalline sample from this "border-line" range. Apart from the unavoidable inhomogeneous broadening (and the fact that $\alpha(T)$ presents a polycrystalline average), qualitative agreement with the corresponding single-crystal results (fig. 3a) is noted.

To summarize the findings on CeCu_2Si_2 , a new HF ground state with magnetic signatures occurs in Ce/Cu deficient samples. This so-called phase A develops out

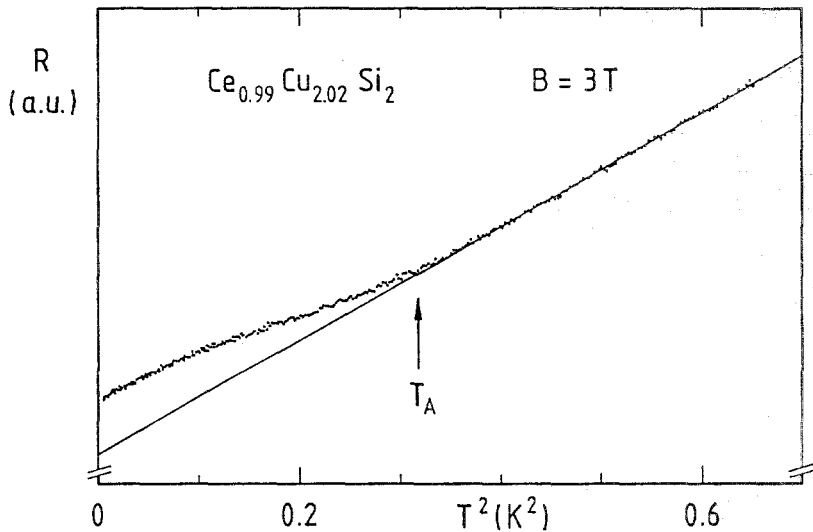


Fig. 5. Electrical resistance (in arbitrary units) of a polycrystalline $\text{Ce}_{0.99}\text{Cu}_{2.02}\text{Si}_2$ sample (from “phase-A” regime, cf. fig. 4) as a function of T^2 at $B = 3 \text{ T}$. Arrow marks transition from paramagnetic phase C into phase A.³⁶

of the coherent heavy-Fermi-liquid state and gives rise to additional scattering, as displayed in fig. 5. Its transition temperature T_A limits, by as yet unknown reasons, the highest possible superconducting T_c .^{32,37} HF superconductivity and phase A compete for stability, i.e. they do not coexist on a microscopic scale. This behavior contrasts with the one of the actinide-based HF metal UPd_2Al_3 for which coexistence of two different ground-state properties is found, as will be discussed in the subsequent section.

4. COEXISTENCE OF HEAVY-FERMION SUPERCONDUCTIVITY AND ANTIFERROMAGNETISM IN UPd_2Al_3

This most recently discovered HF superconductor²⁸ exhibits a strongly anisotropic magnetic susceptibility, $\chi(T)$, in the paramagnetic state.⁴¹ Above $T_N = 14 \text{ K}$, $\chi_{\perp c}/\chi_{\parallel c} \simeq 3$, where $\chi_{\perp c}$ is the susceptibility measured when the B field is applied along the basal plane, while $\chi_{\parallel c}$ marks the susceptibility for B applied parallel to the hexagonal c axis. Owing to a large specific-heat, $C(T)$, anomaly at $T = T_N$ a sizeable ordered moment was inferred.²⁸ In fact, neutron-diffraction experiments on both polycrystalline²⁹ and single-crystal samples⁴² reveal $\mu(T \rightarrow 0 \text{ K}) = \mu_0 = 0.85 \mu_B$. The magnetic moments being aligned ferromagnetically within the basal planes are stacked along the c axis in a simple type-I antiferromagnetic order. Except for a small anomaly (not only in the intensity, but also in the width of the $(00\frac{1}{2})$ magnetic Bragg reflection), the ordered moment appears

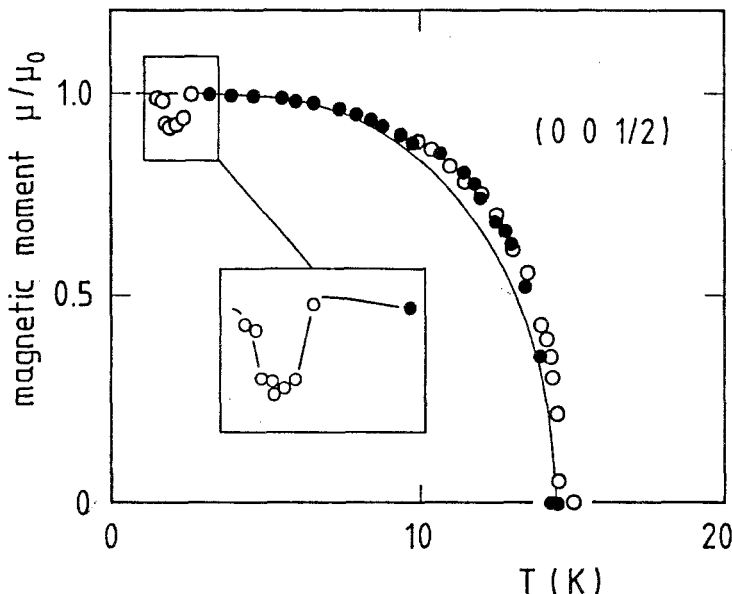


Fig. 6. Temperature dependence of the reduced ordered moment for the strongest magnetic Bragg peak ($00\frac{1}{2}$) of a UPd_2Al_3 single crystal. For comparison, a $S = \frac{1}{2}$ Brillouin function is also shown. Open and full circles correspond to the results of experiments performed at two different spectrometers. Inset: T-dependence of the integrated intensity of the ($00\frac{1}{2}$) peak near T_c (adapted from⁴³).

unaffected by the onset of superconductivity at $T_c = 2$ K (fig.6). This indicates that the two phenomena are only weakly interacting with each other and, further on, that they coexist in a homogeneous way - as was independently concluded from μSR results.⁴⁴ No gap in the electronic (as well as in the magnetic) excitation spectrum has been detected for UPd_2Al_3 .^{45,46} Polarized-neutron studies (performed in the paramagnetic state for $B \perp c$) have shown unequivocally that the magnetic moments are localized at the U sites, with no measurable transfer of magnetization density to Pd.⁴⁷ However, when compared to results of static-, bulk-magnetization measurements, about 15% of the field-induced moment was found to be missing at the U site and was presumed to be transferred to itinerant electronic states.⁴⁷

UPd_2Al_3 shows a bulk superconducting phase transition at $T_c = 2$ K, the highest value for any HF superconductor at ambient pressure.²⁸ It represents the rare case of a very clean type-II superconductor, with an extremely large Ginzburg-Landau parameter $\kappa \simeq 50$. For polycrystalline material, the quasiparticle transport mean free path was estimated to be $\ell \simeq 700$ Å, exceeding the Ginzburg-Landau coherence length, $\xi_0 = 85$ Å, by nearly one order of magnitude. The electronic

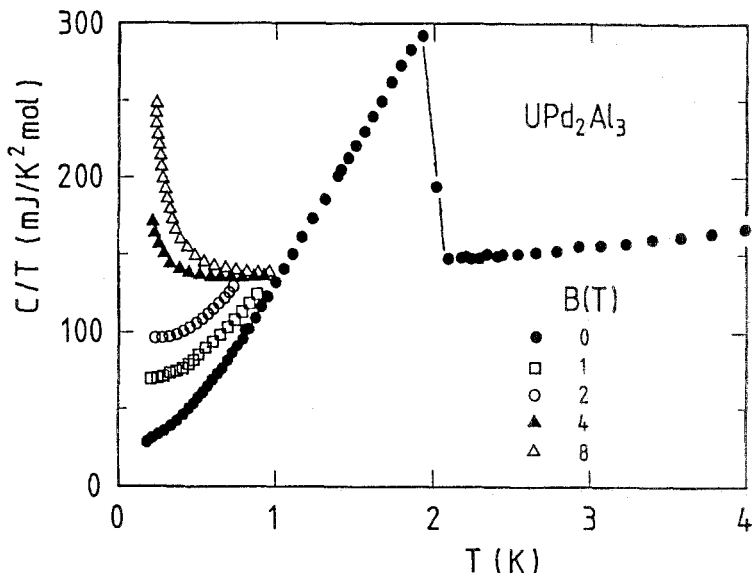


Fig. 7. Specific heat of polycrystalline UPd_2Al_3 as C/T vs T at zero magnetic field, in the mixed state ($B = 1\text{ T}, 2\text{ T}$) as well as in the normal state ($B = 4\text{ T}, 8\text{ T}$). Extrapolation to $T = 0\text{ K}$ of the $B = 0\text{ T}$ data yields (i) $\gamma \approx 140\text{ mJ/K}^2\text{ mole}$ for $T \gtrsim T_c = 2\text{ K}$ and (ii) $\gamma_r = 25\text{ mJ/K}^2\text{ mole}$ for $T < 1\text{ K}$. The quasiparticle contribution of the superconductor is $\gamma_s = \gamma - \gamma_r \approx 115\text{ mJ/K}^2\text{ mole}$.⁴⁵

normal-state specific heat, γT , in the magnetically ordered state is as large as in a prototypical LMM compound like CeAl_2 :⁶ $\gamma = 140\text{ mJ/K}^2\text{ mole}$. The $C(T)$ discontinuity at T_c is of the same size as the large value of γT_c (cf. fig. 7); such a giant specific-heat jump being one of the hallmarks of a HF superconductor. Further support for Cooper pairs formed by heavy (slow) quasiparticles derives from the large negative slope of $B_{c2}(T)$ at T_c , -4.3 T/K .^{28,44} In the following, we mention several additional properties considered characteristic for a HF superconductor: (i) a T^3 power-law quasiparticle contribution to the specific heat in the superconducting state is found for $T < 1\text{ K}$ (fig. 7), in agreement with results of thermal-expansion experiments.⁴⁸ (ii) Metallic point contacts between UPd_2Al_3 and tungsten yield an unusual Andreev-reflection spectrum,⁴⁹ similar to what was previously observed for URu_2Si_2 ^{50,51} and UPt_3 .^{52,51} (iii) When dopant atoms with a valence different from that of the corresponding constituent in the host compound are alloyed into UPd_2Al_3 , a strong T_c depression is noticed. Independent on the lattice site involved in this doping, superconductivity becomes completely suppressed, once the transport mean free path is reduced to the size of the coherence length: $\ell \approx \xi_0$.⁵³ This

important result may be taken as evidence for a highly anisotropic superconducting order parameter, $\Delta(\mathbf{k})$. Whether $\Delta(\mathbf{k})$ is vanishing at points or along lines on the Fermi surface remains to be unravelled: in contrast to the T^3 law resolved in the low- T specific heat (fig. 7), a quadratic temperature dependence of $(T_1T)^{-1}$ was obtained from the NQR-derived spin-lattice relaxation rate,³⁰ in agreement with earlier NMR results.⁵⁴

We now address the interesting question, how HF superconductivity which is carried by heavy Cooper pairs (formed by weakly delocalized 5f electrons) and antiferromagnetic order between seemingly local 5f-derived moments can coexist on a microscopic scale. To this end we briefly recall results of (a) specific-heat measurements performed under hydrostatic pressure, p ,⁴⁵ and (b) Knight-shift measurements.⁵⁵

The central finding of the specific-heat experiments was that, under application of $p \simeq 11$ kbar, the "residual" ($T \ll T_c$) linear specific-heat term, γ_r , was raised by nearly the same amount as was the Sommerfeld coefficient, γ , of the total electronic specific heat in the normal state ($T \gtrsim T_c$). This remarkable result enables one to separate from the data a p -independent contribution $\gamma_s = \gamma(p) - \gamma_r(p) \simeq 115$ mJ/K²mole. Caspary et al.⁴⁵ have ascribed γ_r (found to be mainly of intrinsic origin⁵⁶) and γ_s to different "subsets" of 5f electrons, a "magnetic" and a "superconducting" one. This assignment is supported by the following observations: (i) The 5f-derived entropy at the magnetic ordering temperature is strongly reduced under pressure, pointing to a corresponding reduction of the staggered moment. (ii) Recent high-pressure experiments by the Geneva group⁵⁷ indicate for $p \leq 65$ kbar a significant T_N depression ($dT_N/dp = -0.09$ K/kbar, in good agreement with a thermodynamic estimate for $p \rightarrow 0$ kbar⁵⁸). (iii) The superconducting T_c does merely not change in this same pressure range.⁵⁷ (iv) The specific-heat jump height at T_c is unaffected by pressures $p \leq 11$ kbar.⁴⁵

Feyerherm et al.⁵⁵ observed a reduction of the muon Knight shift below T_c , being the larger the lower the external magnetic field. Their finding supports earlier conclusions, drawn from the ²⁷Al-NMR Knight shift⁵⁹ and a strongly Pauli-limited $B_{c2}(T)$ curve,⁴⁴ that the HF superconductor UPd₂Al₃ belongs to the even-parity variety. Analyzing their data, the authors obtain the interesting result that the contribution to the 5f-derived susceptibility χ_{5f} , which disappears well below T_c (as $B \rightarrow 0$ T), is nearly isotropic: $\chi_{5f}^{\text{"band''}} = (2.0 \pm 0.4) \cdot 10^{-3}$ emu/mole. This enables one to separate from the total $\chi_{5f}(T)$ a T -independent, strongly anisotropic contribution, $\chi_{5f}^{\text{"local''}} = \chi_{5f} - \chi_{5f}^{\text{"band''}}$. These two different contributions to χ_{5f} are, again, ascribed to the "magnetic" and "superconducting" subsets of 5f states, respectively.⁵⁵

Caspary et al.⁴⁵ estimated from their entropy results that the fraction of "superconducting" 5f states $f_s \simeq 0.5$. Furthermore, these states can be characterized, within a Kondo-lattice picture, by $T_{\text{high}}^* \geq 25$ K. On the other hand, we may compare the "magnetic" 5f states to a prototypical LMM system like CeAl₂. Here, the measured value of $\gamma_r \simeq 140$ mJ/K²mole amounts to $\simeq 10\%$ of the Sommerfeld coefficient, γ_p , as expected for fictitious paramagnetic CeAl₂ ($T^* = 4$ K, nearly coinciding with T_N).⁶ Choosing for UPd₂Al₃ the corresponding ratio, $\gamma_r/\gamma_p = (1 - f_s) \cdot 0.1$, we estimate $T_{\text{low}}^* \simeq 14$ K which is close to T_N for this compound, too.

To summarize, LMM type of antiferromagnetic ordering and HF superconductivity coexist in UPd_2Al_3 in a homogeneous manner (at least on a scale of the superconducting coherence length). As argued above, such a coexistence is not possible for a Kondo-lattice system, i.e. in the one-parameter-scaling scheme first introduced by Doniach.⁶⁰ We conclude from this fact that the valence state of U in UPd_2Al_3 cannot be U^{3+} ; for, such a Kramers ion must retain a magnetic ground state in the presence of crystal-field (CF) splitting. In fact, the T-dependencies of the anisotropic susceptibility⁴¹ as well as of the specific heat⁶¹ and recent doping experiments,⁵³ strongly favor a tetravalent (non-Kramers, $5f^2$) state of uranium. A combined analysis of $\chi(T)$ and $C(T)$ has led to a CF-level scheme that contains two low-lying singlet states (32 K apart from each other) and two excited doublets (Γ_5 and Γ_6 , 109 K and 168 K above the CF ground state, respectively).⁶¹ Within this CF-level scheme, the large $5f$ moment would have to be of the “induced” type. A theoretical investigation is needed to clarify whether antiferromagnetic ordering between induced local $5f$ moments and HF superconductivity can coexist homogeneously within the “ U^{4+} scenario”.

An alternative description may start by comparing recent band-structure calculations by Sandratskii et al.⁶² with dHvA results by Inada et al.,⁶³ who were able to monitor five extremal cross sections of the Fermi surface, with effective masses ranging from $10m_0$ to $33m_0$. Several extremal orbits, i.e. those associated with the heaviest masses ($m^* \lesssim 70m_0$)^{28,37} could not yet be detected. The fundamental frequencies of the experimentally observed extremal orbits are accurately calculated based upon the local approach to the spin-density functional,⁶² while the effective band masses come out to be much smaller than the experimental values.⁶³ Interestingly enough, Sandratskii et al.⁶² are able to also calculate the staggered moment very accurately ($\mu_0 = 0.87\mu_B$ as compared to the experimental value of $0.85\mu_B$). Therefore, it appears justified to consider both the “magnetic” and “superconducting” $5f$ states in UPd_2Al_3 itinerant from the outset. The fact that present band-structure calculations are not in the position to obtain the large quasiparticle masses indicates its inability to properly take into account the on-site Coulomb correlations which are responsible for the dramatic mass renormalization at low temperature. Within this “itinerant picture”, both subsets of $5f$ electrons have to be considered as “localized” on nearly disjunct portions of the Fermi surface. Their quite different T^* values estimated within the Kondo-lattice approach, may then correspond to quite different hybridization strengths of the U-derived $5f$ states with Pd-/Al-states. In fact, two Fermi surface sheets, well separated from each other, one consisting of pure U-states, the other one showing substantial admixture of Pd- and Al- to U-states, have been obtained theoretically.⁶² In contrast to the classical Chevrel-phase superconductors, where magnetic and superconducting electrons are residing on different sublattices and are, thus, spatially well separated from each other, our hypothesis invokes that for UPd_2Al_3 the magnetic and superconducting $5f$ states are nearly separated in k-space rather than in r-space. The reasons for such a “k-space localization” need to be explored by future work. In this context we wish to recall the extremely weak interaction between antiferromagnetism and HF superconductivity inferred both from doping⁵³ and pressure⁵⁷ experiments.

5. PERSPECTIVE

Lanthanide-based HF metals belong to the class of (either magnetically ordered or non-magnetic) Kondo lattices. They can be classified by a single coupling parameter and contain localized $4f$ electrons in both the LMM and the weak-coupling high-temperature/high-field state. However, in the strong-coupling regime of the coherent heavy Fermi liquid the $4f$ electrons are itinerant, i.e. they contribute to the Fermi surface. Residual interactions between the heavy quasiparticles can result in different symmetry-broken states. For the exemplary compound CeCu_2Si_2 it was found that, depending on the actual stoichiometry in the vicinity of the “122” phase, single crystals usually adopt one of two competing ground states: HF superconductivity and the magnetic phase A. As our investigation of polycrystalline material with differing composition shows, these phases are almost degenerate in an extremely narrow composition range. The B-T phase diagram for samples out of this “border-line” range reveals non-overlapping existence regimes of the two different states. In particular, for external fields $B < B_{c2}$ an incipient formation of phase A is observed upon cooling. Below $T = T_c(B)$, HF superconductivity expels the phase A. In such samples, the thermodynamic stability of the superconducting state appears to be markedly weakened. The transition temperature T_A (at $B = 0$ T) limits the highest possible superconducting T_c . Determination of the different symmetries of these competing ground states is left as a topic of great importance. In polycrystalline samples of CeCu_2Si_2 , up to three different domains occur simultaneously in a heterogeneous way. Similar “multi-domain” effects have been discovered before for CeAl_3 .⁶⁴

By contrast, our exemplary actinide-based HF metal, UPd_2Al_3 , exhibits coexistence of a seeming LMM state and HF superconductivity in homogeneous samples. Being not allowed for a Kondo lattice of f -ions with magnetic ground state, this coexistence may be explained under special circumstances if an (integer) valence $4+$, i.e. a non-Kramers $5f^2$ configuration, of uranium is assumed. Alternatively, the $5f$ electrons in this as well as in other U-based HF metals may be considered itinerant from the outset. Although direct $5f$ -wavefunction overlap is safely prevented in all of these materials, strong hybridization with ligand states may result in delocalized $5f$ states; owing to their spatial extent which exceeds considerably that of the $4f$ states. This “itinerant scenario” naturally implies a non-integer valence of U (being very likely intermediate between $4+$ and $3+$). Consequently, simple one-parameter scaling is then not applicable to classify the ground-state properties of U-based HF metals. Let us recall, in this context, that there exist several phenomenological differences in microscopic probes when comparing U- and Ce-based HF metals, which otherwise behave quite similarly in bulk properties.⁵ In contrast to their Ce-counterparts, none of the U-compounds shows an indication either (i) of the intra-atomic Coulomb repulsion energy, U_{ff} , in photo-electron spectroscopy⁶⁵ or (ii) of CF-splitting effects in inelastic neutron-scattering spectra,^{66,49} though Schottky-type anomalies have occasionally been resolved in specific-heat data.^{67,61} Finally, low-temperature Shubnikov-de-Haas measurements on UPt_3 performed as a function of external magnetic field have revealed no measurable change in Fermi-surface volume on raising the field from $B < B_m$ to $B > B_m$, $B_m \simeq 20$ T being the metamagnetic field of this compound.⁶⁸ Whereas at sufficiently high field, the

4f electrons in CeRu₂Si₂ localize,¹⁴ the 5f electrons in UPt₃ appear to remain itinerant.⁶⁹

To conclude, the nature of the low-energy excitations in the class of U-based HF metals remains an open issue: It is of great interest to understand which mechanism (potentially different from the ordinary Kondo effect) is operative to generate effective carrier masses at low temperature being as "heavy" as in the Ce counterparts. Theory is challenged to explore this "alternative road to heavy-fermion behavior".⁷¹

6. ACKNOWLEDGEMENTS

Stimulating conversations with J.W. Allen, G. Bruls, P. Coleman, D.M. Edwards, H. Eschrig, R. Feyerherm, P. Fulde, K. Gloos, L.P. Gorkov, D. Jaccard, Yu. Kagan, Y. Kitaoka, T. Komatsubara, J. Kuebler, A. Loidl, B. Luethi, E. Mueller-Hartmann, Y. Ōnuki, M. Peter, M. Richter, L.M. Sandratskii, N. Sato, A. Schenck, G. Sparr, D. Vollhardt, G. Zwicknagl and, notably, P. Fazekas are gratefully acknowledged. This work was performed within the research program of the Sonderforschungsbereich 252 Darmstadt/Frankfurt/Mainz.

REFERENCES

1. P. Fulde, this conference.
2. T. Brugger et al., *Phys. Rev. Lett.* **71**, 2481 (1993).
3. P. Fulde et al., *Z. Phys. B* **92**, 133 (1993).
4. T. Kasuya et al., *Physica* **186-188 B**, 9 (1993).
5. N. Grewe and F. Steglich, in: *Handbook on the Physics and Chemistry of Rare Earths*, Vol. 14, K.A. Gschneidner Jr. and L. Eyring (eds.) (Elsevier, Amsterdam, 1991) p.343.
6. C.D. Bredl et al., *Z. Phys. B* **29**, 327 (1978).
7. C.D. Bredl, *J. Magn. Magn. Mat.* **63 & 64**, 355 (1987).
8. K. Kadowaki and S.B. Wood, *Solid State Commun.* **58**, 507 (1986).
9. W. Joss et al., *Phys. Rev. Lett.* **59**, 1609 (1987).
10. G.G. Lonzarich, *J. Magn. Magn. Mat.* **76 & 77**, 1 (1988).
11. M. Springford and P.H.P. Reinders, *ibid.*, p. 11.
12. L.C. Gupta et al., *Phys. Rev. B* **28**, 3673 (1983).
13. Y. Ōnuki et al., *J. Phys. Soc. Jpn.* **53**, 1210 (1984). G.R. Stewart et al., *Phys. Rev. B* **30**, 482 (1984).
14. H. Aoki et al., *Phys. Rev. Lett.* **71**, 2110 (1993).
15. G. Zwicknagl, *Adv. Phys.* **41**, 203 (1992).
16. R. Felten et al., *J. Magn. Magn. Mat.* **63-64**, 383 (1987).
17. M.A. Continentino, *Phys. Rev. B* **47**, 11587 (1993-I).
18. H. von Loehneysen et al., *Phys. Rev. Lett.* **72**, 3262 (1994).
19. F. Steglich et al., *J. Low Temp. Phys.* **95**, 3 (1994).
20. D. Jaccard et al., *Phys. Lett. A* **163**, 475 (1992).
21. A. Loidl et al., *Ann. Phys. (Leipzig)* **1**, 78 (1992).
22. F. Steglich et al., *Phys. Rev. Lett.* **43**, 1892 (1979).
23. G. Aeppli et al., *J. Magn. Magn. Mat.* **76 & 77**, 385 (1988).
24. J. Sauls, *Adv. Phys.* **43**, 113 (1994).
25. C. Broholm et al., *Phys. Rev. Lett.* **58**, 1467 (1987).
26. C. Geibel et al., *Z. Phys. B* **83**, 305 (1991).

27. J.G. Lussier et al., *Physica B* **199-200**, 137 (1994).
28. C. Geibel et al., *Z. Phys. B* **84**, 1 (1991).
29. A. Krimmel et al., *Z. Phys. B* **86**, 161 (1992).
30. Y. Kitaoka et al., *Physica B* (in press).
31. R. Feyerherm et al., *Physica B* (in press).
32. M. Lang et al., *Physica Scripta T* **39**, 135 (1991).
33. G. Bruls et al., *Phys. Rev. Lett.* **72**, 1754 (1994).
34. B. Andraka et al., *Phys. Rev. B* **48**, 3939 (1993).
35. T.C. Kobayashi et al., *Physica B* (in press).
36. P. Gegenwart, unpublished results.
37. F. Steglich et al., *Physica C* **185-189**, 379 (1991).
38. R. Modler et al., *Physica B* (in press).
39. H. Spille et al., *Helv. Phys. Acta* **56**, 165 (1983).
40. M. Ishikawa et al., *J. Magn. Magn. Mat.* **63 & 64**, 351 (1987).
41. A. Grauel et al., *Phys. Rev. B* **46**, 5818 (1992).
42. H. Kita et al., *J. Phys. Soc. Jpn.* **63**, 726 (1994).
43. A. Krimmel et al., *Solid State Commun.* **87**, 829 (1993).
44. A. Amato et al., *Europhys. Lett.* **19**, 127 (1992).
45. R. Caspary et al., *Phys. Rev. Lett.* **71**, 2146 (1993).
46. M. Dressel et al., *Physica B* **199-200**, 173 (1994).
47. L. Paolasini et al., *J. Phys.: Cond. Mat.* **5**, 8905 (1993).
48. K. Gloos et al., *Phys. Rev. Lett.* **70**, 501 (1993).
49. F. Steglich et al., *Physica C* (in press).
50. K. Hasselbach et al., *Phys. Rev. B* **46**, 5827 (1992-I).
51. Y. de Wilde et al., *Phys. Rev. Lett.* **72**, 2278 (1994).
52. G. Goll et al., *Phys. Rev. Lett.* **70**, 2008 (1993).
53. C. Geibel et al., *Physica B* (in press).
54. Y. Kitaoka et al., *Physica B* **186-188**, 229 (1993).
55. R. Feyerherm et al., *Phys. Rev. Lett.* **73**, 1849 (1994).
56. P. Hellmann, unpublished results.
57. P. Link et al., to be published.
58. R. Modler et al., *Int. J. Mod. Phys. B* **7**, 42 (1993).
59. M. Kyogaku et al., *Physica B* **186-188**, 285 (1993).
60. S. Doniach, *Physica* **91B**, 231 (1977).
61. A. Boehm et al., *Int. J. Mod. Phys. B* **7**, 34 (1993).
62. L.M. Sandratskii et al., *Phys. Rev. B* **50** (1 December 1994).
63. Y. Inada et al., *Physica B* **119-120**, 119 (1994).
64. S. Barth et al., *Phys. Rev. Lett.* **59**, 2991 (1987).
65. J.W. Allen et al., *Phys. Rev. Lett.* **54**, 2365 (1985).
66. A.I. Goldmann et al., *Phys. Rev. B* **33**, 1627 (1986).
67. R. Felten et al., *Europhys. Lett.* **2**, 323 (1986).
68. S.R. Julian et al., *Phys. Rev. B* **46**, 9821 (1992-I).
69. Note that UPd₃, the only U-based intermetallic known to contain localized 5f states, is not a HF metal.⁷⁰
70. See, e.g.: J.W. Allen et al., *Physica B* **186-188**, 307 (1993).
71. See, e.g.: K. Penc and A. Zawadowski, *Phys. Rev. B* **50** (15 October 1994).